Available online at www.sciencedirect.com

ScienceDirect

Procedia Manufacturing 43 (2020) 2–9

Procedia MANUFACTURING

www.elsevier.com/locate/procedia

17th Global Conference on Sustainable Manufacturing

A Decision Method to Improve the Sustainability of Post Processing in Multi Jet Fusion Additive Manufacturing

Mattia Mele[a], Giampaolo Campana[a,*], Gian Luca Monti[b]

[a] *University of Bologna, Viale del Risorgimento 2,40136 Bologna, Italy*
[b] *Studio Pedrini, Via Persicetana Vecchia 7/6, 40132 Bologna, Italy*

Abstract

The improvements in terms of sustainability achievable by means of additive manufacturing processes have been widely investigated in the literature. Nevertheless, less information exists on the economic, societal and environmental impacts of the post-processing phase of additively manufactured parts. The present paper analyses the case of sandblasting in Multi Jet Fusion process chain. The main impact factors of this operation are examined to show their importance on the sustainability of the production. The thermal bleeding defect is deepened, due to its high influence. A descriptor to aid the decision-making about build orientation is proposed and applied to a real case.

© 2020 The Authors. Published by Elsevier B.V.
This is an open access article under the CC BY-NC-ND license (http://creativecommons.org/licenses/by-nc-nd/4.0/)
Peer review under the responsibility of the scientific committee of the Global Conference on Sustainable Manufacturing.

Keywords: Multi Jet Fusion; Thermal-bleeding; Post process; Additive Manufacturing

Nomenclature

$\hat{N}_i$	Normal vector of the i-th triangular element
$n_{i,z}$	Z-direction component of $\hat{N}_i$
N_θ	Number of steps in inclination angle
N_ϕ	Number of steps in azimuth angle
$\hat{d}_i(\phi,\theta)$	Unitary vector with polar coordinates ϕ,θ in the local coordinate system of the i-th triangle
$L_i(\phi,\theta)$	Minimum non-null intersection in the direction $\hat{d}_i(\phi,\theta)$
D_i	Heat disposal index of the i-th triangle
TBR_i	Thermal bleed risk index of the i-th triangle
A_i	Area of the i-th triangle
N_t	Number of triangles of the part

* Corresponding author. Tel.: +39 051 2093456 ; fax: +39 051 2093412.
E-mail address: giampaolo.campana@unibo.it

2351-9789 © 2020 The Authors. Published by Elsevier B.V.
This is an open access article under the CC BY-NC-ND license (http://creativecommons.org/licenses/by-nc-nd/4.0/)
Peer review under the responsibility of the scientific committee of the Global Conference on Sustainable Manufacturing.
10.1016/j.promfg.2020.02.101

P_{tb}	Penalty thermal bleeding factor of the part

1. Introduction

1.1. Multi Jet Fusion process

The peculiar features of Additive Manufacturing (AM) technologies offer new opportunities to improve the sustainability of industrial production [2]. In particular, the overcoming of many limitations connected to traditional processes enables to design products with reduced environmental, economic and societal impact in their life-cycle [3, 11].
These opportunities may be taken extending the applications of these technologies to large scale industrial productions [21]. In this direction, one of the main limitations comes from the low production rate of many AM technologies if compared to traditional processes [16].
High-Speed Sintering (HSS) [20] aims to overcome the productive limitations of Selective Laser Sintering (SLS). The improvement in speed of HSS is obtained by dropping a carbon black-based agent on a layer of Poly-Amide (PA) and then fusing the material by means of Infra-Red (IR) radiation [4]. This approach has been demonstrated to also improve the mechanical performances of manufactured parts, thus enlarging the applicability in industrial field [1].
Multi Jet Fusion (MJF) is a powder bed process patented by HP in which a surfactant (named *detailing agent*) is deposited at the borders of carbon black to improve the accuracy of each layer; the layer is then fused by means of IR radiation provided by moving lamps [8]. The characteristics of manufactured parts and the extremely high production rate of MJF make it a strategic technology for the large-scale application of AM [17, 15]. At the end of the process, the building station has to be cooled down to guarantee the dimensional stability of manufactured parts before they are removed from the non-fused powder. 80% of the powder is recycled for the next processes.

1.2. Post-Processing and sustainability

As in the other powder-based processes, parts need to be cleaned and finished before being applied. A combination of bead blasting and air blasting is an obligatory step for parts produced via MJF in order to remove the remaining powder attached to the part after removal from the building station [12]. The abrasive element suggested by HP are glass [12] or a mix of glass beads and graphite [13], nevertheless, different media can be efficiently adopted. The part can be then be subjected to further finishing methods; for example, ultrasonic cavitation [19], magnetic abrasion [6] have been recently proposed in the literature for the finishing of AMed parts.

The main resources consumption and pollution per minute of blasting are reported in Tab 1 according to the results presented by [18].

The increase of blasting time has, therefore, a direct effect on Global Warming Potential (GWP), Acidification Potential (AP), Water Eutrophication Potential (WEP), Resource Depletion Potential (RDP) and Respiratory Inorganics (RI) [18].
To reach an adequate level of finishing, the bead blasting has to be manually performed [12]. During this phase, the operator is subject to healthy risks [7], that might be mitigated by means of adequate practices [5]. The unergonomic position of the operator during blasting (depending on the adopted equipment) also results in musculoskeletal fatigue when maintained for long periods. Furthermore, the blasting phase is mainly perceived as tedious and frustrating by operators, thus resulting in a low satisfaction of workers; this is even truer when a long time is spent on a single area as in the case of thermal bleeding.
As blasting has an average consumption of 1.4 kg of glass beads per hour [12], the increase in post-processing time directly reflects on the cost of the whole process; this is even more evident if the amount of energy consumed during the operation and machine amortisation are included. The need to perform the operation manually has also a strong impact on the cost of the product that is directly related to the cost of work. The duration of post-processing is thus fundamental in order to contain the costs of the production and enabling a fast response to market requests (that is one

Table 1. Resources consumption and pollution of blasting per minute (adapted by [18])

Pollution type	Resource of pollution	Amount (kg/min)
Atmospheric emission	CO2	1.54E-01
	CH4	4.43E-04
	HCL	4.21E-05
	HF	5.26E-06
	SO2	4.53E-04
	NOX	4.28E-04
	Particles PM2.5	1.45E-06
	Inhalable particles	4.21E-07
Water emission	Ammonia nitrogen	3.23E-07
	Nitrate	6.04E-09
	Phospate	1.43E-08
Resource consumption	Coal	1.01E-01
	Natural gas	5.85E-05
	Crude oil	1.70E-04

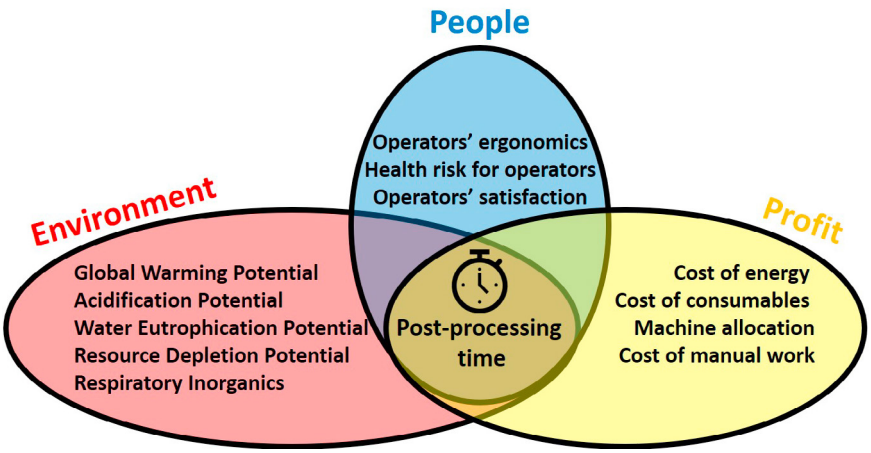

Fig. 1. Fields of impacts proportional to post-processing time

of the main features of AM technologies).
Fig. 1 summarises the main voices of the impact that have a direct correlation with the post-processing time.

1.3. Thermal bleeding

The parts produced via MJF are affected by some peculiar defects that can be avoided or mitigated through an appropriate design of the part and process [10].

In particular, a characteristic defect named thermal bleeding occurs when heat surrounding parts is not efficiently disposed of during cooling. This leads to the undesired local sintering of white powder as shown in Fig. 2

The risk of thermal bleeding is related to different factors, including irradiance of the fusing lamps, the volumetric density of the build job, the distance between parts, part design, part orientation and eventual hardware issues. These influential factors are briefly explained in the following.

The irradiance of the fusing lamps in MJF process has to be set according to the volumetric density of the build job, i.e. to the ratio between the volume of fused material and the total volume of deposited powder. An excess in energy provided by means of irradiance may result in a heat accumulation with the consequent appearing of thermal bleeding.

As well, high values of volumetric density or an insufficient distance between parts may lead to the localised accumu-

Fig. 2. Example of thermal bleeding on a part manufactured via MJF

lation of heat and thus to the undesired sintering of white powder adjacent to parts. These aspects are connected to the nesting of the build platform and thus to production planning.
Looking at the single part, the design of massive parts is also a critical factor for the risk of thermal bleeding, as a higher amount of heat has to be disposed to reach environment temperature.
During platform cooling, the heat tends to flow upward, especially when fast cooling methods are adopted to shorten the production time [9]. For this reason, the part orientation plays a crucial role in determining the probability of thermal bleed to arise on the part. In particular, down-facing concave surfaces enclosing massive volumes are more exposed to the risk of defect's arising. Therefore, acting on the orientation of parts is an effective way to reduce or eliminate the defect.

As the exceeding powder must be removed to obtain the desired part, thermal bleeding leads to a severe increase of post-processing time. In fact, during blasting, the operator must remain on the affected zone for a long time in order to abrade the white powder sintered to the part. In the hardest cases, the sandblasting action of beads is not sufficient to remove the coating powder, that has to be mechanically scrapped.

As described in the previous sections, a direct proportion exists between the blasting time and the sustainability of the entire manufacturing cycle. Therefore, the increase of post-processing time due to thermal bleeding is directly proportional to the impact of the entire production cycle. Avoiding or reducing the amount of sintered extra powder is thus fundamental in order to enhance the sustainability of production.

In the following, an index for the prediction of thermal bleeding seriousness is derived. This indicator can be used to compare alternative manufacturing solutions and drive decision-making in the direction of sustainability. A comparative analysis of a real part with two different build orientations is used to demonstrate the potential benefits of the prosed method.

2. Method

To predict the probability of thermal bleeding on part surfaces, a topological descriptor has been developed using as a starting point the triangles of the STL file. This descriptor aims to include the features relevant to the risk of thermal bleeding (according to what described in 1.2), i.e.:

- Orientation of the surface
- Capability of the part to efficiently dispose of the heat
- Mass of the part below the surface

In STL codification, the generic i-th triangular element is described by means of twelve single-precision floating-point values, i.e. the nine spatial coordinated of the three vertices and the three components of the unitary vector $\hat{N}_i$ normal to the surface (also represented in 3).

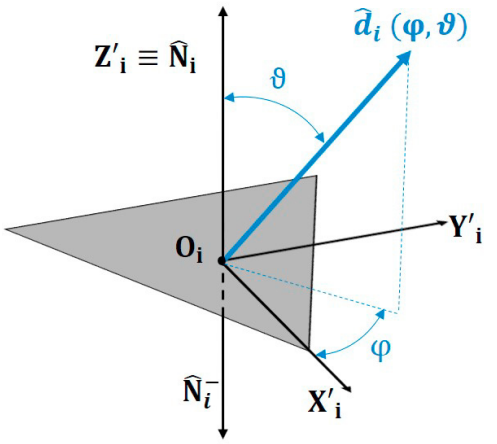

Fig. 3. Representation of local coordinate system of the generic triangle and outgoing vector

The component along Z-direction of the vector $\hat{N}_i$ ($n_{i,z}$) is in the range [-1;+1] and provides an immediate indication about the orientation of the surface. In fact, high values of $n_{i,z}$ indicate up-facing elements with a reduced probability of thermal bleeding, while negative values belong to down-facing triangles having a high risk of showing the defect.
To describe the capability of the surface to dispose of heat, a ray-casting-based approach has been used sending rays with different directions from the centre O_i of the i-th triangle. The generic unitary vector with polar coordinates ϕ and θ in a local coordinate system having Z'-Axis coincident with the normal of the triangle (as shown in 3) will be indicated as $\hat{d}_i(\phi,\theta)$ in the following. Sending a ray from O_i along $\hat{d}_i(\phi,\theta)$ direction and using a ray casting algorithm [14] to check intersections with the other triangles of the mesh, the minimum non-null distance $L_i(\phi,\theta)$ is obtained; in case no intersection is found with other triangles, the distance to the platform walls along $\hat{d}_i(\phi,\theta)$ is used .

To describe the capability of the i-th element to dispose heat, we divide the inclination angle in N_θ steps and the azimuth in N_ϕ and calculate $L_i(\phi,\theta)$ for the corresponding $d_i(\phi,\theta)$ directions. Using these assumptions, it is possible to define the index $D_i(\phi,\theta)$ as in Eq. 1 :

$$D_i(N_\phi,N_\theta)=\sum_{j=1}^{N_\phi}\sum_{k=1}^{N_\theta}\frac{L_i(j\frac{2\pi}{N_\phi},\pi-k\frac{\pi}{2N_\theta})}{L_i(j\frac{2\pi}{N_\phi},k\frac{\pi}{2N_\theta})} \tag{1}$$

This index is inversely proportional to the capability of the surface to dispose of heat. The mapping of space used in Eq. 1 leads to having a higher number of vectors near to normal, thus giving more influence to these directions in the calculation of $V_i(N_\phi$; this is coherent with the preferential heat exchange direction of the surface.
A high value of the numerator in Eq. 1 indicates a sufficient distance from any other element in a given direction, while low values are characteristic of surfaces with a reduced capability of heat disposal.

The denominator of 1 quantifies the amount of material below the surface in the given direction, that is directly related to the amount of heat to be disposed of.

Therefore, for each combination of j and k, a high value of the addendum in Eq. 1 contributes to increase the risk of thermal bleed.

To take into account the orientation of the surface, the thermal bleeding risk factor of the generic i-th element (TBR_i) can be thus calculated as in 2

$$TBR_i = D_i(1-n_{i,z}) \tag{2}$$

For sake of simplicity, the numbers N_θ and N_ϕ of angular steps have been assumed to be fixed and omitted in Eq. 2. It is worth noticing that the value of TBR_i goes to zero when the normal of an element is coincident to the Z-axis (being this the best-case scenario for element orientation).

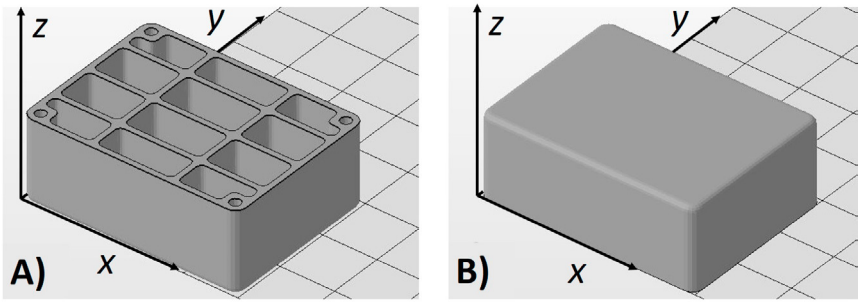

Fig. 4. Part used for the comparison between orientation A) and B)

Finally, the time required for bead blasting depends on the extension of thermal bleeding, i.e. of regions to be hardly finished. Therefore, we can define a penalty factor P_{tb} associated to the thermal bleeding of the part (in a datum orientation) as the sum for the N_t triangles of the coefficient TBR_i multiplied by the area of the i-th triangle A_i, as expressed in Eq. 3

$$P_{tb} = \sum_{i=1}^{N_t} TBR_i A_i \tag{3}$$

The index P_{tb} can be thus used during part orientation in order to minimise the severity and extension of areas affected by thermal bleeding, thus reducing the time required for bead blasting and improving the sustainability of the entire process. In the next section, two different orientations of the same part are compared to show the potential benefits achievable through a prediction of thermal bleeding in the production planning phase.

3. Results and discussion

The case in Fig. 4 has been used for the validation of the method. The model consists of 4420 triangles, with a bounding box of 40 x 30 x 15 mm, a volume of 5.9 cm^3 and a total surface of 103.2 cm^2. The part has been manufactured with building orientations A and B in Fig. 4 by means of an HP Jet Fusion 4200 working in fast mode. PA12 was used as material for the parts. The results have been compared in order to evaluate the effectiveness of the index in forecasting the severity of thermal bleeding and, as a consequence, impacts on process sustainability.

The index P_{tb} has been measured equal to 1.988 E10 in orientation A and equal to 7.600 E09 in orientation B. Therefore, the application of the method here proposed leads to prefer orientation B for manufacturing.

Both the parts have been given to the same operator for post-processing and the corresponding time has been measured by means of a chronometer. A pressure of 4 bars was used for sandblasting using corundum. Fig. **??** shows the two parts after 1 minute and 20 seconds of sandblasting.

As can be seen, the thermal bleeding effect is clearly visible in the part printed with orientation A, while the part with orientation B already reached the desired quality of finish. To remove the extra powder and reach the same surficial quality, extra 16 minutes and 10 seconds of sandblasting were necessary. This confirms the huge influence of thermal bleeding on post-processing times and the effectiveness of the proposed index in predicting the more sustainable manufacturing solution.

Considering a batch size of 1200 parts to be produced, a comparison of impacts is given in Tab 2. The Global Warming Potential (GWP), Acidification Potential (AP), Water Eutrophication Potential (WEP) and Respiratory Inorganics (RI) indicators are calculated according to the allocation factors reported by [18].

As it can be observed in Tab. 2, a total saving of 10 hours can be obtained on the entire production. It is worth mentioning that all the 1200 cases can be nested in a single build job, thus the entire batch production can be manufactured in approximately 12 hours (excluding the cooling time). Therefore, the achieved reduction in post-processing time leads to a significant decrease in delivery time. Considering an approximate cost of 35 €/h for sandblasting

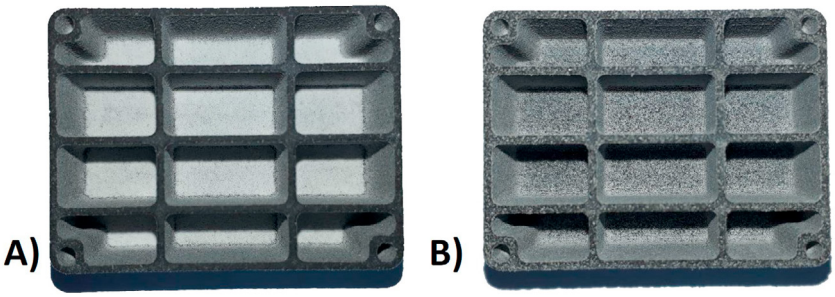

Fig. 5. Parts printed with orientation A) and B) after 1 minute and 20 seconds of sandblasting

Table 2. Comparison of impacts for two different orientation of part

Quantity	Orientation A	Orientation B	Unit
P_{tb}	1.988 E10	7.600 E09	mm^2
Post-processing time per part	17:30	01:20	mm:ss/part
Total post-processing time	350:00	26:40	hhh:mm
Estimated post-processing cost	12250	933	€
Global Warming Potential (GWP)	3.47E+03	2.64E+02	kg CO2 eq
Acidification Potential (AP)	1.68E+01	1.28E+00	kg SO2 eq
Water Eutrophication Potential (WEP)	2.55E-03	1.94E-04	kg NO3 eq
Respiratory Inorganics (RI)	7.77E-01	5.92E-02	kg PM2.5 eq

(including the cost of the operator), direct saving of 11'317€ can be achieved orienting the case as in Fig. 4 B).
Looking at Tab. 2 it is also possible to notice how all the environmental indicators decrease of an order of magnitude in the second solution.
It is worth mentioning how all these values are proportional to the number of parts so that the described advantages become even more evident for larger production batches.

4. Conclusions

The relevance of post-processing in determining the sustainability of AM and, in particular, the MJF process has been discussed. The role of thermal bleeding was deepened, underlining the influence of this defect on the post-processing time.
To drive the decision-making in the direction of sustainability a new index for the prediction of thermal bleed severity has been derived. This indicator can be used to compare different manufacturing solutions, choosing the one with the minimum impact coming from the post-processing phase.

The proposed approach has been applied to a real case study in order to point out the effectiveness of the proposed index in predicting the part with the lower post-processing time. Furthermore, the quantification of savings in terms of time, cost and environmental impacts pointed out the benefits achievable operating the right choices during the design of the process.

The results underline the importance of reducing the impacts of the post-processing phase of AM processes in order to enhance their sustainability. For this scope, the development of predictive comparative tools is fundamental to aid the decision-making before the production take place.

Acknowledgements

The authors would like to thank the MIUR (Italian Ministry of University and Research) for the financial support to the present work.

References

[1] Craft, G., Nussbaum, J., Crane, N., Harmon, J.P., 2018. Impact of extended sintering times on mechanical properties in PA-12 parts produced by powderbed fusion processes. Additive Manufacturing 22, 800–806. URL: https://doi.org/10.1016/j.addma.2018.06.028, doi:10.1016/j.addma.2018.06.028.

[2] Despeisse, M., Ford, S., Despeisse, M., Ford, S., Role, T., Resource, I., 2017. The Role of Additive Manufacturing in Improving Resource Efficiency and Sustainability To cite this version : HAL Id : hal-01431086 Resource Efficiency and Sustainability .

[3] Diegel, O., Kristav, P., Motte, D., Kianian, B., 2016. Additive Manufacturing and its Effect on Sustainable Design, Springer, Singapore, pp. 73–99. URL: http://link.springer.com/10.1007/978-981-10-0549-7{_}5, doi:10.1007/978-981-10-0549-7_5.

[4] Ellis, A., Noble, C.J., Hopkinson, N., 2014. High Speed Sintering: Assessing the influence of print density on microstructure and mechanical properties of nylon parts. Additive Manufacturing 1, 48–51. URL: http://dx.doi.org/10.1016/j.addma.2014.07.003, doi:10.1016/j.addma.2014.07.003.

[5] Goodier, J.L., Lucas, E.B., Coletta, R., 1974. Industrial Health and Safety Criteria for Abrasive Blast Cleaning Operations. Arthur D. Little. Inc. Cambridge. Massachusetts , 1–61.

[6] Guo, J., Au, K.H., Sun, C.N., Goh, M.H., Kum, C.W., Liu, K., Wei, J., Suzuki, H., Kang, R., 2019. Novel rotating-vibrating magnetic abrasive polishing method for double-layered internal surface finishing. Journal of Materials Processing Technology 264, 422–437. URL: https://doi.org/10.1016/j.jmatprotec.2018.09.024, doi:10.1016/j.jmatprotec.2018.09.024.

[7] Horowitz, M.R., Hallock, M.F., 2019. RECOGNITION OF HEALTH HAZARDS IN THE WORKPLACE, in: Handbook of Occupational Safety and Health. John Wiley & Sons, Inc., Hoboken, NJ, USA, pp. 1–36. URL: http://doi.wiley.com/10.1002/9781119581482.ch1, doi:10.1002/9781119581482.ch1.

[8] HP Development Company L.P., 2014. HP Multi Jet Fusion technology. Technical White Paper , 8.

[9] HP Development Company L.P., 2017a. Fast Cooling Functionality. Technical White Paper , 3–5URL: http://h10032.www1.hp.com/ctg/Manual/c05358991.

[10] HP Development Company L.P., 2017b. Multi Jet Fusion printing tips and tricks. Technical White Paper .

[11] Joshi, S.C., Sheikh, A.A., 2015. 3D printing in aerospace and its long-term sustainability. Virtual and Physical Prototyping 10, 175–185. URL: http://www.tandfonline.com/doi/full/10.1080/17452759.2015.1111519, doi:10.1080/17452759.2015.1111519.

[12] L.P., H.D.C., 2017a. Air Blasting Process General overview. Technical White Paper .

[13] L.P., H.D.C., 2017b. Manual Graphite Blasting Executive summary Applications for MJF printed parts Test / post-process overview. Technical White Paper .

[14] Moller, T., Trumbore, B., 1998. Fast, minimum storage ray-triangle intersection. Doktorsavhandlingar vid Chalmers Tekniska Hogskola , 109–115doi:10.1080/10867651.1997.10487468, arXiv:arXiv:1011.1669v3.

[15] Morales-Planas, S., Minguella-Canela, J., Lluma-Fuentes, J., Travieso-Rodriguez, J.A., García-Granada, A.A., 2018. Multi Jet Fusion PA12 manufacturing parameters for watertightness, strength and tolerances. Materials 11, 1–11. doi:10.3390/ma11081472.

[16] Ngo, T.D., Kashani, A., Imbalzano, G., Nguyen, K.T., Hui, D., 2018. Additive manufacturing (3D printing): A review of materials, methods, applications and challenges. Composites Part B: Engineering 143, 172–196. URL: https://doi.org/10.1016/j.compositesb.2018.02.012, doi:10.1016/j.compositesb.2018.02.012.

[17] O'Connor, H.J., Dickson, A.N., Dowling, D.P., 2018. Evaluation of the mechanical performance of polymer parts fabricated using a production scale multi jet fusion printing process. Additive Manufacturing 22, 381–387. doi:10.1016/j.addma.2018.05.035.

[18] Peng, S., Li, T., Tang, Z., Shi, J., Zhang, H., 2016. Comparative life cycle assessment of remanufacturing cleaning technologies. Journal of Cleaner Production 137, 475–489. URL: http://dx.doi.org/10.1016/j.jclepro.2016.07.120, doi:10.1016/j.jclepro.2016.07.120.

[19] Tan, K.L., Yeo, S.H., 2017. Surface modification of additive manufactured components by ultrasonic cavitation abrasive finishing. Wear 378-379, 90–95. URL: http://dx.doi.org/10.1016/j.wear.2017.02.030, doi:10.1016/j.wear.2017.02.030.

[20] Thomas, H.R., Hopkinson, N., Erasenthiran, P., 2006. High Speed Sintering – Continuing Research into a New Rapid Manufacturing Process. Proceedings of the 17th Solid Freeform Fabrication Symposium (SFF) , 682–691URL: http://sffsymposium.engr.utexas.edu/2006TOC{%}0Ahttp://sffsymposium.engr.utexas.edu/Manuscripts/2006/2006-59-Thomas.pdf.

[21] Tofail, S.A., Koumoulos, E.P., Bandyopadhyay, A., Bose, S., O'Donoghue, L., Charitidis, C., 2018. Additive manufacturing: scientific and technological challenges, market uptake and opportunities. Materials Today 21, 22–37. URL: https://doi.org/10.1016/j.mattod.2017.07.001, doi:10.1016/j.mattod.2017.07.001.